Title

7-hydroxytropolone is the main metabolite responsible for the fungal antagonism of *Pseudomonas donghuensis* strain SVBP6

Authors

Federico Matías Muzio[1], Betina Cecilia Agaras[1], Marco Masi[2], Angela Tuzi[2], Antonio Evidente[2], Claudio Valverde[1*]

Affiliation

[1] Laboratorio de Fisiología y Genética de Bacterias Beneficiosas para Plantas – Centro de Bioquímica y Microbiología del Suelo. Departamento de Ciencia y Tecnología. Universidad Nacional de Quilmes - CONICET.

Roque Sáenz Peña 352, Bernal B1876BXD, Buenos Aires, Argentina.

[2] Dipartimento di Scienze Chimiche, Università di Napoli "Federico II", Complesso Universitario Monte Sant'Angelo, Via Cintia 4, 80126 Naples, Italy.

* **Author for correspondence**

Tel.: +54-11-4365-7100 ext. 5638. Fax: +54-11-4365-7132. E-mail: cvalver@unq.edu.ar, valverdecl@hotmail.com

Running title: 7HT, an antifungal metabolite of *P. donghuensis*

This article has been accepted for publication and undergone full peer review but has not been through the copyediting, typesetting, pagination and proofreading process which may lead to differences between this version and the Version of Record. Please cite this article as doi: 10.1111/1462-2920.14925

Originality-Significance statement

Our study revealed, for the first time, that 7-hydroxytropolone (7HT) is the major extracellular compound responsible for the broad antifungal activity of *Pseudomonas donghuensis* strain SVBP6. It positions 7HT as a novel secondary metabolite with fungal inhibitory activity among the chemical arsenal of *Pseudomonas* species with biocontrol traits.

Summary

Pseudomonas donghuensis strain SVBP6, an isolate from an agricultural plot in Argentina, displays a broad-spectrum and diffusible antifungal activity which requires a functional *gacS* gene but could not be ascribed yet to known secondary metabolites typical of *Pseudomonas* biocontrol species. Here, we report that Tn*5* mutagenesis allowed the identification of a gene cluster involved in both the fungal antagonism and the production of a soluble tropolonoid compound. The ethyl acetate extract from culture supernatant showed a dose-dependent inhibitory effect against the phytopathogenic fungus *Macrophomina phaseolina*. The main compound present in the organic extract was identified by spectroscopic and X-ray analyses as 7-hydroxytropolone (7HT). Its structure and tautomerism was confirmed by preparing the two key derivatives 2,3-dimethoxy- and 2,7-dimethoxy-tropone. 7HT, but not 2,3- or 2,7-dimethoxy-tropone, mimicked the fungal inhibitory activity of the ethyl acetate extract from culture supernatant. The activity of 7HT, as well as its production, was barely affected by the presence of up to 50 μM added iron (Fe^{+2}). To summarize, *P. donghuensis* SVBP6 produces 7HT under the positive control of the Gac-Rsm cascade

and is the main active metabolite responsible for the broad-spectrum inhibition of different phytopathogenic fungi.

Keywords: *Pseudomonas donghuensis*; antifungal activity; 7-hydroxytropolone; *Macrophomina phaseolina*.

Introduction

The rhizosphere microbiome of healthy plants harnesses plant beneficial bacteria with the ability to inhibit the growth of fungal plant pathogens by means of production of secondary metabolites with fungicidal or fungistatic activity (Mendes et al., 2011). This implies one major mechanism for biological control (or biocontrol) of potentially harmful agents for plants, which complements the ability of other rhizobacteria to induce systemic resistance (Lugtenberg and Kamilova, 2009). Taxonomically relevant biocontrol groups that are ubiquitous constituents of the rhizosphere microbiome include members of the Bacillales, Burkholderiales, Actinobacteria, and of the *Pseudomonas* genus (Mendes et al., 2011; Ciancio et al., 2019; Mullins et al., 2019; Newitt et al., 2019; Zhou et al., 2019). In particular, due to their ease to isolate, metabolic versatility, genomic attributes and the wealth of available genetic tools, diverse *Pseudomonas* species (*e.g.*, *P. protegens*, *P. fluorescens* and *P. chlororaphis*) have been broadly characterized as prominent biocontrol representatives of the microbiome of different plant species (Haas and Defago, 2005; Loper et al., 2012). The exploitation of these culturable species for management of fungal diseases can be boosted by elucidating the chemical compounds responsible for the biocontrol activity, and by characterizing the underlying metabolic and molecular regulatory mechanisms.

We have recently isolated from an agricultural soil in Argentina, strain SVBP6 – a member of the recently defined *Pseudomonas donghuensis* species (Jiang et al., 2016)- as a bacterium with a remarkable broad-spectrum *in vitro* antifungal activity (Agaras et al., 2015; Agaras et al., 2018), which is due to diffusible, but not volatile, compounds (Agaras et al., 2018). A thorough mining of SVBP6 draft genome did not reveal obvious gene clusters related to production of soluble secondary metabolites typical of other biocontrol pseudomonads, such as 2,4-diacetylphloroglucinol, pyrrolnitrin, pyoluteorin, cyclic or linear lipopeptides, phenazines, 2-hexyl 5-propyl resorcinol, or mupirocin (Haas and Keel, 2003; Loper et al., 2012; Paterson et al., 2017; Biessy et al., 2019). We observed, however, that alike production of most of the aforementioned compounds, the antagonistic activity of strain SVBP6 is strongly dependent on the Gac-Rsm global regulatory system (Lapouge et al., 2008; Agaras et al., 2018). In this context, the goal of this work was the identification of the compound(s) responsible for the *in vitro* fungal antagonism displayed by *P. donghuensis* SVBP6, by a combination of genetic, physiological and chemical approaches.

Results

Identification of a gene cluster involved in fungal antagonism.

In order to get insights into the molecular basis underlying the broad antifungal activity displayed by *P. donghuensis* strain SVBP6, we screened a Tn*5* mutant library (Agaras et al., 2018) for clones showing a strong reduction in the *in vitro* antagonism against a local isolate of the fungal phytopathogen *Macrophomina phaseolina* (Table

S1). Among a set of nearly 60 selected mutants with reduced antagonism for which the Tn*5* insertion site was determined, we found 6 independent clones whose Tn*5* hits mapped close to each other within a 16-kb region in scaffold 5.1 of the SVBP6 draft genome (Figure 1). This region comprises 3 genes encoding a putative efflux transport system, a set of 9 genes encoding metabolic enzyme functions, and 2 genes encoding transcriptional regulators of the LysR and TetR families (Figure 1, Table 1). Based on *in silico* operon prediction, it appears that gene expression in this region would be organized into three polycistronic transcripts, namely *orf4-orf5-orf6-orf7*, *orf11-orf10-orf9-orf8*, and *orf12-orf13* (Figure 1). This is supported by the location and direction of predicted promoters (Figure 1).

[Place Figure 1 here]

Every predicted protein within this 16-kb region shows a level of identity of at least 99% with proteins encoded by the genomes of the two other published *P. donghuensis* strains, HYS and P482 (Gao et al., 2012; Krzyzanowska et al., 2014). Outside the *Pseudomonas* genus, the putative operon *orf4-7* encodes proteins with highly identical orthologs (75-78%) present in members of the proteobacterial species *Stenotrophomonas rhizophila* and *Collimonas* sp. (Table 1); the putative operon *orf12-13* encodes orthologs of *Pseudoduganella violaceinigra* (a member of the Burkholderiales), whereas the putative operon *orf11-8* encodes proteins with a variable level of identity (55-73%) with orthologs of members of α-, β- and γ-proteobacteria (Table 1). Within the *Pseudomonas* genus, the whole gene cluster has been detected with a high degree of conservation and syntenic arrangement in the genomes of a set of only 15 strains among a total of 528 complete and 8578 draft genomes available at the

Pseudomonas Genome DB (http://www.pseudomonas.com/: December 2019) (Figure S1). On the basis of their 16S rDNA sequences, the strains harbouring the orthologous cluster are representatives of *P. donghuensis* (HYS, P482, Irchel 3F5, 1239, ABAC8, NBRC 111117, RIT263), *P. qingdaonensis* (JJ3, BIGb0473, PA14H7, 1033, MF6396, BRM28, UASWS0946), and *P. wadenswilerensis* (SNU WT1), being the three of them recently described species within the broad *P. putida* group (Gao et al., 2015; Frasson et al., 2017; Wang et al., 2019) (Figure S1). Recently, the corresponding region of strain HYS has been implicated in the biosynthesis of 7-hydroxytropolone (7HT), which apparently serves this strain as an iron scavenging compound (Jiang et al., 2016; Chen et al., 2018). The high level of gene and protein sequence identity within this locus between strains HYS and SVBP6, as well as the fact that at least *orf11* shows a strong identity with the *tdaD* gene reported as essential for the production of tropodithietic acid in several marine bacteria of the *Roseobacter* clade (including *Phaeobacter* spp.; Table 1) (Geng et al., 2008; Wang et al., 2016), strongly suggests a genetic linkage between the SVBP6 cluster involved in fungal antagonism (Figure 1) and the production of a tropolonoid molecule.

Strain SVBP6 produces a soluble compound compatible with 7HT

Because 7HT has a characteristic UV absorption pattern (Jiang et al., 2016), we obtained the UV-visible spectrum of the culture filtrates of strain SVBP6 and its isogenic mutants after 8 h of growth in KB medium. As shown in Figure 2a, the supernatant from wild type SVBP6 contains the two hallmark maximum absorption peaks of 327 nm and 393 nm reported for 7HT, with an A327/A393 absorptivity ratio of

1.6 (Jiang et al., 2016). However, the supernatant of mutant 16d, which lost antifungal activity, does not show the UV absorption peaks of SVBP6 supernatant (Figure 2a).

A similar pattern was observed for the rest of the Tn*5* mutants mapped in the region shown in Figure 1 (Figures 2b, 2c). Interestingly, the supernatant of a *gacS*::Tn*5* clone from our library, previously reported as unable to inhibit 12 different phytopathogenic fungal isolates (Agaras et al., 2018), also lost the UV peaks of the wild type SVBP6 supernatant (Figures 2a, 2b, 2c). In line with this observation, we found three sequences within the locus shown in Figure 1, which upon being transcribed may serve as targets for the post-transcriptional regulatory cascade Gac-Rsm (Figure 1). One of these putative target sequences maps in the 5'-UTR region of the putative operon *orf11-8*, for which 3 Tn*5* hits were detected in this study (Figure 1).

[Place Figure 2 here]

At the microscopic level in co-culture PDA plates, the effect of the compounds diffusing out from SVBP6 streaks is evidenced as a sharp front of densely packed hyphae that cannot progress further towards the bacterial streak, although there are no obvious alterations in the morphology of individual hyphal filaments of the phytopathogenic fungus *M. phaseolina* isolate CCC 131.2010 (Table S1; Figure S2). Similar observations were obtained for two other fungal plant pathogens and for the oomycete *Pythium ultimum* (Table S1; data not shown). Both the inactivation of *gacS* or *orf10* (mutant 16d) restored the normal density of hyphae and avoided formation of the sharp front of inhibition (Figure S2). Strain SVBP6 also displays a diffusible and Gac-Rsm dependent inhibitory activity against *Bacillus subtilis* and *Escherichia coli* (Agaras et al., 2018). However, all the Tn*5* mutants that lost the ability to restrict growth of

different fungi and that did not produce the UV-absorbing compound still retained their antibacterial activity (Figure 2c, Figure S3).

When we monitored the UV absorption at 327 nm and 393 nm of the culture supernatant along the growth of strain SVBP6 in KB medium, we found that production of the tropolonoid compound is induced at mid exponential phase and reaches a maximum level in early stationary phase after 7-8 h of culture (Figure 2d), whereas the characteristic UV peaks are almost undetectable in the supernatant of the *gacS*::Tn*5* mutant all along the growth curve (Figure 2d). When cultures were let growing for 30 h, we observed the presence of a greenish fluorescent pigment compatible with pyoverdine, for both the wild type strain and the *gacS*::Tn*5*, as well as for all the mutant clones mapped in the 16-kb locus of scaffold 5.1, except for mutant 83j (Figure 2c). This was reflected in the UV spectrum of the culture supernatants as an appearance of a typical peak with an absorption maximum around 400 nm (Xiao and Kisaalita, 1995) (Figure S4a). However, in the wild type strain, the pyoverdine peak was superimposed to that of the tropolonoid compound in the same region, thus resulting in a mixed pattern that reduced the wild type A327/A393 absorptivity ratio from 1.6 to 1.1 (Figure S4a).

To summarize, strain SVBP6 produces a soluble compound compatible with 7HT (or a closely related species), which reaches a maximum concentration in KB medium at the end of the exponential phase and whose production requires an operative Gac-Rsm cascade, expression of genes from the putative operons *orf4-7* and *orf11-8*, and expression of at least the TetR-transcriptional regulator gene *orf14* (Figures 1 and 2). SVBP6 also produces pyoverdine in late stationary phase cultures in KB medium, although it is not dependent on the Gac-Rsm cascade or genes required for biosynthesis of the tropolonoid compound (Figure 2). Mutations that result in loss of production of

the tropolonoid compound also abolish the inhibitory activity of *P. donghuensis* SVBP6 against different fungi, but not its antibacterial activity (Figure 2c; (Agaras et al., 2018)).

Extraction of the fungal metabolites with inhibitory activity from SVBP6 culture supernatants

An ethyl acetate (EtOAc) extract was obtained from the culture supernatant of the wild type strain grown in KB for 8 h. The EtOAc extract retained the characteristic UV pattern of the wild type culture supernatant (Figures 2a, 3a). The EtOAc extract was then used to test its ability to inhibit the growth of *M. phaseolina* in a microplate assay developed in this study (Figure 3b). In the absence of added EtOAc extract, the cell-free supernatant of SVBP6, but not that of mutant 16d, delayed the growth of *M. phaseolina* (Figures 3b, 3c). Similar results were observed with *Fusarium graminearum* strain CCC 122-2010 and *F. semitectum* strain CCC 120-2010 (Figure S5). These results are in line with the fact that SVBP6 –but not mutant 16d- generates a growth inhibition halo against different fungi in dual plate assays (Figure 2c; (Agaras et al., 2015; Agaras et al., 2018)).

[Place Figure 3 here]

When the EtOAc extract was incorporated into the cell-free culture supernatant of mutant 16d, the A327 of the complemented supernatant resembled that of the SVBP6 culture supernatant (Figure 3a) and the growth inhibition against *M. phaseolina*, *F. graminearum* and *F. semitectum* was restored (Figures 3b, 3c, S5). The same effect was

observed when the EtOAc extract was added to sterile KB medium (which served as a control for the culture supernatants) (Figures 3b, 3c, S5). Moreover, when the EtOAc extract was added to the cell-free supernatant from SVBP6 cultures, the strength of *M. phaseolina* inhibition was clearly increased (Figures 3b, 3c). Altogether, these results indicate that: 1) the EtOAc extract retains the UV pattern of the culture supernatant suggesting that the tropolonoid compound is present in the extract; 2) the metabolites with inhibitory activity against *M. phaseolina* and other fungal phytopathogens present in the extracellular medium of strain SVBP6 are also extracted with EtOAc; 3) the EtOAc extract complements the inhibitory defect of a supernatant from mutant 16d; 4) the EtOAc extract appears to display a dose-response effect.

Dose-inhibition curve and stability of the active metabolites contained in the EtOAc extract

On the basis of the observation described in the previous section (Figure 3), we carried out a dose-response assay to test the inhibitory activity of the EtOAc extract when added to sterile KB medium at a range of doses around average concentrations found in the supernatant of SVBP6 cultures in late exponential phase. The content of the tropolonoid compound present in every tested dose of the EtOAc was monitored by UV spectrophotometry (Figure 4a). As shown in Figure 4, there was a positively correlated strength in the inhibition of *M. phaseolina* growth with the increasing dose of EtOAc added to the test wells (Figures 4b, 4c).

[Place Figure 4 here]

We noticed that in this type of *in vitro* inhibition assay in which there are no live bacterial cells, but only their extracellular products, *M. phaseolina* can finally override the inhibition set by the compound(s) present at the start of the experiment in either the culture supernatant (Figure 3b) or the EtOAc extract (Figure 4b), and resume growth after an initial dose-dependent delay. This is in sharp contrast to what we have consistently observed in co-culture inhibition assays in PDA plates with bacterial streaks and fungal mycelium (Agaras et al., 2015; Agaras et al., 2018), in which an inhibition zone is established and the fungus can never reach the bacterial streak (Figure S2), therefore defining a restricted zone of filament growth that remains for at least 4 weeks at 28 °C.

To explore whether the "overriding" phenomenon in the absence of live cells may be due to an intrinsic chemical instability of the inhibitory compound(s), we evaluated the residual antifungal activity of a fixed amount of EtOAc extract incorporated into PDA by delaying the inoculation of *M. phaseolina* once a day for up to 5 days (Figure 4d). The experiment revealed that the inhibitory activity remaining in the agarized medium at the moment of fungal inoculation had dropped to about 50% of the initial amount after 5 days of incubation without the fungus (Figure 4d). Such loss of activity represents a daily average reduction of 10%. With this decay rate, for an initial EtOAc extract dose of 4×, there still should be enough inhibitory compound(s) after 5 days of incubation (*i.e.*, 50% or an equivalent of EtOAc extract dose of 2×) to impose a larger delay in the growth of *M. phaseolina* than the one detected for the 4× dose (Figure 4d). Thus, we conclude that the intrinsic chemical instability of the tropolonoid compound present in the EtOAc extract from SBVP6 culture supernatant is not enough to explain the overriding capacity of *M. phaseolina*, and it consequently suggests that the fungus may actively metabolize or neutralize the inhibition present in

the EtOAc extract in the absence of SVBP6 live cells replenishing the inhibitory compound (as it happens in dual culture tests confronting fungi and bacteria). The possibility that the phytopathogenic fungus *M. phaseolina* uses active defence or escape mechanisms to cope with the toxic bacterial metabolite is also suggested by the very striking morphology of the fungus (dense mycelium) when grown at significant concentrations of the compound (Figure S2). Similar phenotypes have been observed with other compounds of bacterial origin (Garbeva et al., 2014; Aunsbjerg et al., 2015; Torres et al., 2016; Melloul et al., 2018).

Isolation and chemical characterization of 7HT from the EtOAc extract

The culture filtrate of *P. donghuensis* SVBP6 was exhaustively extracted with EtOAc as detailed in the Experimental Procedures section. The crude extract was crystallized with slow evaporation of a hydroalcoholic solution. The single crystal obtained was suitable for X-ray analysis, which unambiguously identified the metabolite as 7HT (Figure 5a). An ORTEP view of 7HT crystal is reported in Figure 5b. The pattern of binding distances unequivocally identified the double bond $C_1 = O_1$ and the position in 2- and 7- of the two OH groups. The hydrogen atoms of the OH groups have been unequivocally identified in the Fourier difference maps and have been freely refined. The crystal structure of 7HT was previously reported by (Kubo et al., 2007), who obtained the parent compound from hydrolysis of 2,7-diacetoxytropone carried out with 50% aqueous acetic acid. The crystal data are reported in Table S1. The structure of 7HT was further confirmed by diazotization reaction, which yielded two dimethyl tautomeric derivatives (Figure 5a) whose ^{1}H NMR data were fully consistent (Figure S6). When the same process was carried out using the organic extract obtained for cell-

free cultures of mutant 16d (Figure 2, Table 1), 7HT was not detected in the TLC (Figure S6).

[Place Figure 5 here]

In summary, the EtOAc extract from the culture supernatant of *P. donghuensis* strain SVBP6, which is inhibitory for the growth of phytopathogenic fungi, contains 7HT (and its tautomer 3HT). By contrast, the supernatant from mutant 16d that is unable to inhibit fungi does not contain 7HT. These observations point to 7HT as the compound responsible for the inhibition of fungal phytopathogens in strain SVBP6.

Purified 7HT, but not 2,3-dimethoxy- or 2,7-demethoxy-tropone, mimics the fungal inhibitory activity of the EtOAc extract from culture supernatant

In order to obtain a definitive confirmation that the inhibitory compound present in the EtOAc extract from culture supernatants of strain SVBP6 is 7HT, we compared the effect on the growth of *M. phaseolina* of equivalent doses of purified 7HT and of the 7HT present in the EtOAc extract (Figure 6a). As shown in Figure 6b, the inhibitory effect of pure 7HT was even slightly stronger than that of the EtOAc extract containing an equivalent amount of 7HT on the basis of its UV spectrum (Figure 6a; *ca*. 12.5 μM in the microplate assay). 7HT was also active against *F. graminearum* and *F. semitectum* (Figure S5).

[Place Figure 6 here]

Furthermore, the inhibitory activity of pure 7HT was completely abolished upon derivatization of both of its hydroxyl moieties, as the growth kinetics of *M. phaseolina* in the presence of either the 2,3-dimethoxy- or the 2,7-dimethoxy-tropone (Figure 5a) was undistinguishable from that of the control treatment (no added compounds) (Figure 6b). These results unambiguously confirm that 7HT is the diffusible inhibitory compound produced by *P. donghuensis* SVBP6, and that the hydroxyl moieties are indispensable for the biological activity of 7HT.

Impact of iron concentration on 7HT production and on inhibition of M. phaseolina

It has been recently reported for *P. donghuensis* strain HYS that 7HT serves to alleviate iron deficiency in the absence of pyoverdine, and that production of 7HT is strongly repressed (>90%) by iron (Fe^{+2}) concentrations of as low as 6-8 µM in the growth medium (Jiang et al., 2016; Chen et al., 2018). Thus, we evaluated the impact of iron supplementation on the production of 7HT by strain SVBP6.

[Place Figure 7 here]

In sharp contrast with the behaviour of strain HYS, production of 7HT in strain SBVP6 was only modestly affected by high ferrous iron concentrations, being reduced to a maximum of *ca*. 50% in the presence of up to 100 µM Fe^{+2} (Figure 7a). These results show that, in contrast to what has been reported for strain HYS (Jiang et al., 2016), production of 7HT in strain SVBP6 is only marginally dependent on iron availability in the growth medium. On the other hand, production of pyoverdine was completely abolished in strain SVBP6 as well as in the *gacS*::Tn*5* mutant when grown

in KB with 30 µM Fe^{+2} (Figure S4b). Yet, considering the claimed role of 7HT as an iron chelating compound (Jiang et al., 2016), we tested the fungal inhibitory activity of the EtOAc extract from SVBP6 culture supernatants in the presence of high iron concentrations. As shown in Figure 7b, when the 7HT concentration was 23 µM, the inhibition of *M. phaseolina* growth was not affected by supplementing Fe^{+2} up to 50 µM. However, for a lower dose of 7HT (12 µM), we detected a slight reduction in the inhibition of *M. phaseolina* growth only for the highest tested iron supplement (50 µM) (Figure 7b), which most likely points to an indirect effect caused by a reduction in the concentration of free 7HT upon formation of the iron:7HT complex (Jiang et al., 2016). Altogether, these results suggest that the production of 7HT in strain SVBP6 –but not of pyoverdine- is mildly sensitive to iron availability, and that the primary inhibitory effect of 7HT against *M. phaseolina* is not the sequestration of iron.

Discussion

The broad-spectrum and diffusible antifungal activity displayed by *Pseudomonas donghuensis* SVBP6 (Agaras et al., 2015; Agaras et al., 2018) draw our attention because genome prospection of SVBP6 did not reveal the presence of gene clusters previously known to be responsible for the biosynthesis of secondary metabolites as reported for several characterized biocontrol pseudomonads (Haas and Keel, 2003; Loper et al., 2012; Paterson et al., 2017; Biessy et al., 2019). There are, however, four orphan genomic regions containing NRPS or hybrid NRPS-PKS orthologs with very low level of similarity to reported clusters, and one additional gene cluster possibly encoding enzymes for production of an arylpolyene (Agaras et al., 2018). Here, with the help of Tn*5* mutagenesis, we identified six independent clones

that lost antagonism against different phytopathogenic fungi and whose Tn*5* insertion sites map within a 16-kb region encoding biosynthetic, regulatory and transport genes (Figure 1); this cluster has been overlooked by *in silico* prospecting tools for secondary metabolite gene clusters in the SVBP6 genome (Agaras et al., 2018). Moreover, a conserved and highly syntenic region seems to be exclusively present in the genomes of *P. donghuensis* strains and of two closely related and recently described species, *P. qingdaonensis* and *P. wadenswilerensis* (Figure S1). This genomic region has been recently associated with the antibacterial activity of *P. donghuensis* strain P482 and with iron scavenging in *P. donghuensis* strains HYS (Krzyzanowska et al., 2016; Chen et al., 2018). Moreover, in the latter strain, the homologous gene cluster was found to be responsible for the production of 7HT (Jiang et al., 2016; Chen et al., 2018). These facts prompted us to query if there was a connection between the antifungal activity of strain SVBP6 and the production of a tropolonoid compound (7HT itself or a closely related molecular species). Our results (Figures 2-7) unequivocally identified 7HT as the main metabolite with fungal antagonism in the culture supernatant of *P. donghuensis* strain SVBP6 and established a link between production of 7HT and the 16-kb gene cluster shown in Figure 1. We cannot rule out the contribution of additional extracellular compounds or enzymes produced by SVBP6, although under the experimental conditions assayed in this work (Figures 2-7), 7HT appears as the major fungal inhibitory metabolite. Tropolones have a unique cyclohepta-2,4,6-trienone moiety, which is a seven-membered non-benzenoid aromatic ring, and they are known to be produced by bacteria, fungi and plants (Guo et al., 2019). α-Hydroxytropolones (like 7HT) are a subgroup of natural tropolonoids that have shown a highly diverse range of biological activity, including antimicrobial, antiviral, and antitumor activities (Meck et al., 2014; Guo et al., 2019).

Which would be antifungal mechanism of 7HT? Previous reports proposed that 7HT could function like a siderophore contributing with iron acquisition in strain HYS (Jiang et al., 2016), and thus suggested competition for iron as a primary mechanistic explanation for the growth inhibition of different fungi observed for strain SVBP6. However, our results strongly discourage such hypothesis for strain SVBP6, because: 1) production of 7HT was not abolished by iron supplementation (as it did happen with pyoverdine production; Figure 2c, Figure S4b); 2) the fungal growth inhibition was not relieved by increasing iron availability (Figure 7); 3) we could not detect DNA sequences consistent with Fur-boxes (Deng et al., 2015) along the promoter regions of the genes and operons annotated in the gene cluster associated with 7HT production in strain SVBP6 (Figure 1). Thus, 7HT most likely acts by an iron-independent mechanism. α-Hydroxytropolones -like 7HT- are heavily oxygenated aromatic compounds consisting in a cycloheptatrienone ring and two free hydroxyls, with all three oxygen atoms in a contiguous array that make them potent competitive inhibitors of a variety of eukaryotic dinuclear metalloenzymes containing divalent ions in their active site, such as Mg^{+2}, Zn^{+2}, and Cu^{+2} (Guo et al., 2019); these include inositol monophosphatase, alkaline phosphatase, dopamine-oxygenase (Meck et al., 2014), as well as of members of the nucleotidyl transferase superfamily requiring two Mg^{+2} ions in their active sites (Piettre et al., 1997). Importantly, the hydroxyl groups of the seven-membered ring of 7HT must not be protected as deprotonation occurs under physiological conditions leading to more efficient chelators (Meck et al., 2014). Our results with the 2,3- and 2,7- dimethoxy-tropones (Figure 6b) are in line with the latter, thus highlighting the importance of the hydroxyl moieties for 7HT activity. Strain SVBP6 produces 7HT as the result of the activity of (at least) the biosynthetic proteins encoded by the identified gene cluster (Figure 1), but in the culture supernatant 7HT is

partially converted into the tautomeric form 3-hydroxytropolone (Figure 5; Figure S6). However, 7HT seems to be the most stable tautomer in solution (Isin and Karakus, 2010), and at a pH near neutrality it would be distributed between its neutral and negatively charged species (Stasiak et al., 2019), which corresponds to the most active chelating form of tropolones (Meck et al., 2014). Altogether, our results and the reported literature on the properties of 7HT strongly let us hypothesize that the broad-spectrum fungistatic activity displayed by strain SVBP6 is the consequence of the competitive inhibition of key non-iron metalloenzymes (Guo et al., 2019).

α-Hydroxytropolones have a broad range of bioactivities, and thus have the potential to serve as a common pharmacophore through which new therapeutics can be developed (Donlin et al., 2017). In particular, the aforementioned excellent metalloenzyme-inhibiting capacity has been the basis for the development of potent inhibitors of various therapeutically important enzymes (Berkowitz et al., 2018). For instance, the chemically synthesized 4-Br-7HT is a potent inhibitor of multidrug resistant *Acinetobacter baumanni* (Cao et al., 2018). However, 7HT is currently produced only chemically by persulfate oxidation of tropolone, but it requires further purification to separate it from the byproducts 5HT, and 3,7- and 4,7-dyhydroxytropolones (Nozoe et al., 1953; Kirst et al., 1982). Thus, bacterial production of 7HT may serve as an alternative source of precursor with sufficient purity for subsequent generation of novel derivatives. In this context, identification of key regulatory factors and the whole set of biosynthetic genes would prompt the design of metabolic engineering strategies for deregulated production of 7HT in *P. donghuensis* strain SVBP6.

Strain SVBP6 is the third reported and sequenced isolate of the recently described species *P. donghuensis* (Gao et al., 2012; Krzyzanowska et al., 2014; Agaras

et al., 2018). The first isolate and type strain HYS was found in the water of the Chinese lake Donghu and it has been characterized as a potent producer of siderophores (Gao et al., 2015), whereas the second isolate P482 was recovered from the rhizosphere of tomato plants in Poland and it showed biocontrol activity against soft rotting bacteria (Krzyzanowska et al., 2014). The genome sequence of the three strains shares a high degree of similarity, with ANI values over 99.5% (Agaras et al., 2018). There are, however, clear evidences of genome specialization: the three strains share a core genome of 4474 genes, but each strain bears an exclusive set of genes (291 for P482, 437 for HYS, and 284 for SVBP6) (Agaras et al., 2018). In the same vein, differential phenotypes have been reported for the three closely related strains. For instance, strain P482 produces volatile compounds that inhibit the growth of fungi (Ossowicki et al., 2017), but strain SVBP6 does not (Agaras et al., 2018); production of 7HT is strongly repressed by <8 μM iron in strain HYS (Jiang et al., 2016), but it is only mildly downregulated in SVBP6 at concentrations as high as 100 μM (Figure 7). Such distinct phenotypic traits may be the result of slightly different evolutionary pressures experienced by each strain within their inhabiting niches. Remarkably, the hallmark phenotype of each of the three strains originated in different continents is linked to the same genomic locus (Figure 1) (Krzyzanowska et al., 2016; Chen et al., 2018), thus suggesting that the biosynthesis of tropolonoid compounds is indispensable for the antibacterial activity of strain P482 (Krzyzanowska et al., 2016), iron scavenging in strain HYS (Jiang et al., 2016; Chen et al., 2018) and the antifungal activity in strain SVBP6.

Concluding remarks

Our study revealed, for the first time, that 7-hydroxytropolone is the major extracellular compound responsible for the broad antifungal activity of *Pseudomonas donghuensis* strain SVBP6. Through a combination of genetic, physiological and chemical analyses, we established a link between the fungal inhibitory activity present in the growth medium of strain SVBP6, 7HT and a 16-kb genetic locus required for its biosynthesis. In brief, we found that 7HT is produced in late exponential phase under the positive control of the Gac-Rsm cascade, and with no major influence of the concentration of iron in the growth medium. 7HT inhibits the growth of different fungi in a dose-response fashion, and its effect is most likely fungistatic. Genes encoding biosynthetic, transport and regulatory functions that are clustered in the identified 16-kb chromosomal region are essential for the production of 7HT and for the broad antifungal activity of strains SVBP6, but not for is antibacterial activity. The two hydroxyl moieties flanking the keto group of 7HT are essential for its activity. These findings demonstrate the benefits of using genome mining and chemical characterizations to define biosynthetic gene clusters associated with a biocontrol trait, and are a key step towards the rationale design of, on the one hand, novel biopesticide formulations for crop production, and on the other hand, of engineered derivatives for overproduction of 7HT as a precursor for novel bioactive tropolonoid compounds.

Experimental Procedures

Microorganisms and culture conditions

The bacterial microorganisms used in this study are listed in Table S1. *P. donghuensis* strain SVBP6 was routinely grown on nutrient agar (NA) or in nutrient yeast broth

(NYB) (Valverde et al., 2003). When required, streptomycin was added to the growth medium (at 100 μg/ml in liquid medium or 200 μg/ml in solid medium). For production of secondary metabolites, strain SVBP6 was grown in King's B medium (King et al., 1954), in Erlenmeyer flasks with rotary agitation (200 rpm) with a 5:1 flask/culture volume ratio. Strain SVBP6 and its isogenic mutants were stored in glycerol 20% at -80 ºC. Routine incubation temperature was 28 °C. Fungal isolates (Table S1) were routinely grown on Potato Dextrose Agar (PDA, Laboratorios Britania) at 28 °C and conidia or microsclerotia suspensions were stored in glycerol 20% at -80 ºC.

*Identification of Tn*5 *mutants with reduced fungal antagonism and determination of the Tn*5 *insertion sites*

The generation of a clone library of random Tn*5* mutants of strain SVBP6 was reported elsewhere (Agaras et al., 2018). Approximately 2500 clones were screened for loss of antagonism against the phytopathogenic fungal isolate *M. phaseolina* CCC 131.2010 (Table S1). Individual clones were streaked onto PDA plates previously overlaid with a suspension of fungal sclerotia and screened after 72 h of incubation at 28 ºC for clones that did not produce a halo of fungal growth inhibition. The Tn*5* insertion sites in the clones of interest were determined by sequencing the amplicons from an arbitrary primed PCR protocol (Martínez-García et al., 2014) at Macrogen Inc. (Seoul, Korea).

In silico tools for DNA sequence and gene function analysis.

The sequence of the gene hit by Tn*5* was identified in every clone of interest by running the BlastN tool (Altschul et al., 1990) of the RAST server (Aziz et al., 2008), using the

DNA sequence flanking the Tn*5* border as a query to interrogate the draft genome of strain SVBP6 (Agaras et al., 2018). Once identified, the predicted protein sequence deduced from every interrupted gene was subjected to homology search analysis through the EBI-HMMER server (Potter et al., 2018) and conserved domain analysis in Pfam (El-Gebali et al., 2019). The DNA sequence of the SVBP6 genomic locus involved in antagonism of fungal isolates was inspected for the presence of promoters with the Bprom (Solovyev and Salamov, 2011) and NNPP (Reese, 2001) servers; Rho-independent terminators were predicted with ARNold (Naville et al., 2011), and co-transcription of predicted ORFs was analyzed with Operon-mapper (Taboada et al., 2018). The DNA pattern tool of the RSAT server was used to search for putative binding sites for the RNA binding proteins of the Csr/Rsm family (Schubert et al., 2007). DNA sequence alignments were carried out with Clustal Omega (Sievers et al., 2011).

In vitro *antagonistic activity of SVBP6 against fungi*

For qualitative analysis of the inhibitory activity of strain SVBP6 and its isogenic Tn*5* mutants, test strains were streaked onto the border region of a PDA plate and a 0.25 cm^2 plug of a fresh fungal culture was deposited onto the centre of the plate. Triplicate plates were incubated for 5 days at 28 °C in the darkness before inspecting for the presence/absence of an inhibition zone in between the bacterial streak and fungal mycelium. Controls without bacteria were included. For time-course quantitative analysis of the inhibition of *M. phaseolina* CCC 131.2010, the 6 wells of a polystyrene plate (Jet Biofil®) were filled each with a total volume of 5 ml of PDA, amended (or not) with cell-free culture supernatants, resuspended organic extracts, or pure

compounds. For this, 2.5 ml of 2× melted PDA was mixed with 2.5 ml of a liquid test sample, just before pouring. Once solidified, an agar plug with a diameter of 2-4 mm from a plate with fresh confluent growth of *M. phaseolina* CCC 131.2010 was gently deposited onto the centre of each agarized well. Plates were sealed with Parafilm, incubated in the dark at 28 °C and photographed at different times to monitor fungal growth. The diameter of the fungal mycelium in each well was measured with Photoshop CC 2019 (Adobe Systems, Inc., San Jose, CA, USA), and used to calculate the fungal growth arbitrary unit (a.u.) defined as the area covered by mycelium relative to the area of the microtiter well.

In vitro *antagonistic activity of SVBP6 against bacteria*

The antibacterial activity of wild type SVBP6 and isogenic Tn*5* mutants was evaluated with the overlay method (Agaras et al., 2018). A 10 µl-drop of a bacterial suspension at OD600 = 1.0 was spotted onto triplicate NA plates, and incubated 24 h at 28°C. Next, the macrocolonies were irradiated with UV for 30 minutes and each plate was overlaid with 4 ml of soft NA (0.8% agar) containing 10% v/v of a saturated culture of the indicator bacterial strain (*Bacillus subtilis*). The overlaid plate was incubated for another 24 h at the optimal temperature of the indicator bacterium (37°C) and inspected for the presence of growth inhibition halos around the irradiated spot.

Extraction of metabolites with inhibitory activity from bacterial culture supernatants

For small-scale organic extract preparations, supernatants were obtained by centrifuging bacterial cultures in KB medium (12,000 rpm for 10 minutes), followed by addition of

1/10 volume of 1 N HCl, and subsequent extraction with 1 volume of ethyl acetate (EtOAc). The extraction was repeated once, and the extracts were pooled. The EtOAc was evaporated in a SpeedVac or a rotary evaporator (depending on the volume) and resuspended in sterile KB medium. The UV-visible spectral properties of the culture supernatants, EtOAc extracts and resuspended material in KB medium, were analyzed with a Nanodrop ND-1000 device.

Purification and chemical characterization of bioactive metabolites

Strain SVBP6 was grown in 1-liter Erlenmeyer flasks containing 250 mL of KB medium. A total of 2 litres of culture supernatant collected at an OD600 of 1.6 were lyophilized. The latter was dissolved in 300 mL of H_2O and extracted at regular pH (7) with EtOAc (3×150 ml). The organic extracts were combined, dried (Na_2SO_4) and evaporated under reduced pressure obtaining an oily residue (84 mg). The residual aqueous phase was acidified to pH 2 with formic acid and extracted with EtOAc (3×150 ml) and the organic extract, processed as above, yielded an oily residue (305 mg). The same procedure was used to extract the lyophilized culture filtrates (50 ml) of mutant strain 16d, obtaining two oily residues (38.6 mg at pH 7 and 2.9 mg at pH 2). The organic extracts were analysed by TLC carried out on silica gel (Merck, Kieselgel 60, F_{254}, 0.25, mm and RP-18 F_{254}, respectively) plates. The spots were visualized by exposure to UV radiation, or by exposure to iodine vapours. An aliquot of the EtOAc organic extract of SVBP6 at pH 7 was dissolved in methanol (MeOH) and some drops of H_2O were added. After 12 h some crystals were obtained and identified as 7-hydroxy tropolone (7HT) by X-ray analysis. For crystal structure determination, a single crystal of 7HT, obtained as above reported, was mounted in flowing N_2 at 173 K in a Bruker-

Nonius KappaCCD diffractometer equipped with Oxford Cryostream apparatus (graphite monochromated Mo Kα radiation λ = 0.71073 Å, CCD rotation images, thick slices, φ and ω scans to fill the asymmetric unit). A semiempirical absorption correction (multiscan, SADABS) was applied. The structure was solved by direct methods using the SIR97 program (Altomare et al., 1999) and anisotropically refined by the full matrix least-squares method on F2 against all independent measured reflections using the SHELXL-2016/6 program (Sheldrick, 2015).

Preparation of 2,3- and 2,7-dimethoxy-tropones

To 7HT (10 mg) dissolved in MeOH (1 ml), an ethereal solution of CH_2N_2 was added to obtain a persistent yellow colour. The reaction was carried out at room temperature and was stopped after 1 h by evaporation under an N_2 stream. The crude residue (10.8 mg) was purified by preparative TLC on silica gel (Merck, Kieselgel 60, F_{254}, 0.5 mm) using $CHCl_3$-*i*-PrOH (9:1) as eluent, to give two main metabolites as amorphous solids. They were identified by ^{1}H NMR spectra which were recorded at 400 MHz in $CDCl_3$ in a Bruker spectrometer. The same solvent was also used as internal standard.

2,3-dimethoxy-tropone: ^{1}H NMR, δ: 7.60 (1H, d, *J* =11.0 Hz, H-4), 7.21 (1H, d, *J* =11.0 Hz, H-7), 7.04 (1H, t, *J* =11.0 Hz, H-6), 6.90 (1H, t, *J*=11.0 Hz, H-5) , 3.96 (3H, s, MeOC-3), 3.93 (3H, s, MeOC-2).

2,7-dimethoxy-tropone: ^{1}H NMR, δ: 6.90 (4H, m, H-3-H-6), 3.95 (6H, m, 2 x OMe).

Acknowledgements

This work was supported by grants from Universidad Nacional de Quilmes (PUNQ 1411/15 and PUNQ 1306/19), CONICET (PIP 11220150100388CO), and by Programme STAR 2017, financially supported by UniNA and Compagnia di San Paolo (grant nr. E62F16001250003). F.M. was supported by a Ph.D. fellowship from CONICET; B.A. and C.V. are members of CONICET. We would like to thank Dr. Andrea Gómez Zavaglia and M.Sc. Gabriel Quintana (CIDCA-UNLP, Argentina), and Sebastián Cavallito (CINDEFI-UNLP, Argentina), for their invaluable support to lyophilize bacterial culture supernatants. We thank Dr. Antonio Lagares Jr. for his critical reading of the manuscript. Authors have no conflict of interest to declare.

References

Agaras, B., Scandiani, M., Luque, A., Fernández, L., Farina, F., Carmona, M. et al. (2015) Quantification of the potential biocontrol and direct plant growth promotion abilities based on multiple biological traits distinguish different groups of *Pseudomonas* spp. isolates. *Biological Control* **90**: 173-186.

Agaras, B.C., Iriarte, A., and Valverde, C.F. (2018) Genomic insights into the broad antifungal activity, plant-probiotic properties, and their regulation, in *Pseudomonas donghuensis* strain SVBP6. *PLoS ONE* **13**: e0194088.

Altomare, A., Burla, M.C., Camalli, M., Cascarano, G.L., Giacovazzo, C., Guagliardi, A. et al. (1999) SIR97: a new tool for crystal structure determination and refinement. *J Appl Crystallogr* **32**: 115-119.

Altschul, S.F., Gish, W., Miller, W., Myers, E.W., and Lipman, D.J. (1990) Basic local alignment search tool. *Journal of Molecular Biology* **215**: 403-410.

Aunsbjerg, S.D., Andersen, K.R., and Knochel, S. (2015) Real-time monitoring of fungal inhibition and morphological changes. *J Microbiol Methods* **119**: 196-202.

Aziz, R.K., Bartels, D., Best, A.A., DeJongh, M., Disz, T., Edwards, R.A. et al. (2008) The RAST Server: rapid annotations using subsystems technology. *BMC Genomics* **9**: 75.

Berkowitz, A.J., Abdelmessih, R.G., and Murelli, R.P. (2018) Amidation Strategy for Final-Step alpha-Hydroxytropolone Diversification. *Tetrahedron Lett* **59**: 3026-3028.

Biessy, A., Novinscak, A., Blom, J., Leger, G., Thomashow, L.S., Cazorla, F.M. et al. (2019) Diversity of phytobeneficial traits revealed by whole-genome analysis of worldwide-isolated phenazine-producing *Pseudomonas* spp. *Environ Microbiol* **21**: 437-455.

Cao, F., Orth, C., Donlin, M.J., Adegboyega, P., Meyers, M.J., Murelli, R.P. et al. (2018) Synthesis and Evaluation of Troponoids as a New Class of Antibiotics. *ACS Omega* **3**: 15125-15133.

Ciancio, A., Pieterse, C.M.J., and Mercado-Blanco, J. (2019) Editorial: Harnessing Useful Rhizosphere Microorganisms for Pathogen and Pest Biocontrol - Second Edition. *Frontiers in Microbiology* **10**.

Chen, M., Wang, P., and Xie, Z. (2018) A Complex Mechanism Involving LysR and TetR/AcrR That Regulates Iron Scavenger Biosynthesis in *Pseudomonas donghuensis* HYS. *J Bacteriol* **200**: e00087-00018.

Deng, Z., Wang, Q., Liu, Z., Zhang, M., Machado, A.C., Chiu, T.P. et al. (2015) Mechanistic insights into metal ion activation and operator recognition by the ferric uptake regulator. *Nat Commun* **6**: 7642.

Donlin, M.J., Zunica, A., Lipnicky, A., Garimallaprabhakaran, A.K., Berkowitz, A.J., Grigoryan, A. et al. (2017) Troponoids Can Inhibit Growth of the Human Fungal Pathogen *Cryptococcus neoformans*. *Antimicrob Agents Chemother* **61**: e02574-02516.

El-Gebali, S., Mistry, J., Bateman, A., Eddy, S.R., Luciani, A., Potter, S.C. et al. (2019) The Pfam protein families database in 2019. *Nucleic Acids Res* **47**: D427-D432.

Frasson, D., Opoku, M., Picozzi, T., Torossi, T., Balada, S., Smits, T.H.M., and Hilber, U. (2017) Pseudomonas wadenswilerensis sp. nov. and Pseudomonas reidholzensis sp. nov., two novel species within the Pseudomonas putida group isolated from forest soil. *Int J Syst Evol Microbiol* **67**: 2853-2861.

Gao, J., Yu, X., and Xie, Z. (2012) Draft genome sequence of high-siderophore-yielding *Pseudomonas* sp. strain HYS. *J Bacteriol* **194**: 4121-4121.

Gao, J., Xie, G., Peng, F., and Xie, Z. (2015) *Pseudomonas donghuensis* sp. nov., exhibiting high-yields of siderophore. *Antonie van Leeuwenhoek* **107**: 83-94.

Garbeva, P., Hordijk, C., Gerards, S., and de Boer, W. (2014) Volatiles produced by the mycophagous soil bacterium Collimonas. *FEMS Microbiol Ecol* **87**: 639-649.

Geng, H., Bruhn, J.B., Nielsen, K.F., Gram, L., and Belas, R. (2008) Genetic dissection of tropodithietic acid biosynthesis by marine roseobacters. *Appl Environ Microbiol* **74**: 1535-1545.

Guo, H., Roman, D., and Beemelmanns, C. (2019) Tropolone natural products. *Nat Prod Rep* **36**: 1137-1155.

Haas, D., and Keel, C. (2003) Regulation of antibiotic production in root-colonizing *Pseudomonas* spp. and relevance for biological control of plant disease. *Annu Rev Phytopathol* **41**: 117-153.

Haas, D., and Defago, G. (2005) Biological control of soil-borne pathogens by fluorescent pseudomonads. *Nat Rev Microbiol* **3**: 307-319.

Isin, D.Ö., and Karakus, N. (2010) Computational study of the intramolecular proton transfer reactions of 3-hydroxytropolone (2,7-dihydroxycyclohepta-2,4,6-trien-1-one) and its dimers. *Journal of Molecular Modeling* **16**: 1877-1882.

Jiang, Z., Chen, M., Yu, X., and Xie, Z. (2016) 7-Hydroxytropolone produced and utilized as an iron-scavenger by Pseudomonas donghuensis. *Biometals* **29**: 817-826.

King, E.O., Ward, M.K., and Raney, D.E. (1954) Two simple media for the demonstration of pyocyanin and fluorescin. *Journal of Laboratory and Clinical Medicine* **44**: 301-307.

Kirst, H.A., Marconi, G.G., Counter, F.T., Ensminger, P.W., Jones, N.D., Chaney, M.O. et al. (1982) Synthesis and characterization of a novel inhibitor of an aminoglycoside-inactivating enzyme. *The Journal of Antibiotics* **35**: 1651-1957.

Krzyzanowska, D.M., Ossowicki, A., and Jafra, S. (2014) Genome Sequence of *Pseudomonas* sp. Strain P482, a Tomato Rhizosphere Isolate with Broad-Spectrum Antimicrobial Activity. *Genome Announc* **2**: e00394-00314.

Krzyzanowska, D.M., Ossowicki, A., Rajewska, M., Maciag, T., Jablonska, M., Obuchowski, M. et al. (2016) When Genome-Based Approach Meets the "Old but Good": Revealing Genes Involved in the Antibacterial Activity of *Pseudomonas* sp. P482 against Soft Rot Pathogens. *Front Microbiol* **7**: 782.

Kubo, K., Matsumoto, T., and Mori, A. (2007) 3-Hydroxytropolone (2,7-dihydroxycyclohepta-2,4,6-trien-1-one). *Acta Crystallographica Section E* **63**: o941-o943.

Lapouge, K., Schubert, M., Allain, F.H., and Haas, D. (2008) Gac/Rsm signal transduction pathway of gamma-proteobacteria: from RNA recognition to regulation of social behaviour. *Molecular Microbiology* **67**: 241-253.

Loper, J.E., Hassan, K.A., Mavrodi, D.V., Davis, E.W., 2nd, Lim, C.K., Shaffer, B.T. et al. (2012) Comparative genomics of plant-associated *Pseudomonas* spp.: insights into diversity and inheritance of traits involved in multitrophic interactions. *PLoS Genet* **8**: e1002784.

Lugtenberg, B., and Kamilova, F. (2009) Plant-growth-promoting rhizobacteria. *Annu Rev Microbiol* **63**: 541-556.

Martínez-García, E., Aparicio, T., de Lorenzo, V., and Nikel, P.I. (2014) New transposon tools tailored for metabolic engineering of gram-negative microbial cell factories. *Frontiers in Bioengineering and Biotechnology* **172**: 46.

Meck, C., D'Erasmo, M.P., Hirsch, D.R., and Murelli, R.P. (2014) The biology and synthesis of alpha-hydroxytropolones. *Medchemcomm* **5**: 842-852.

Melloul, E., Roisin, L., Durieux, M.F., Woerther, P.L., Jenot, D., Risco, V. et al. (2018) Interactions of Aspergillus fumigatus and Stenotrophomonas maltophilia in an in vitro Mixed Biofilm Model: Does the Strain Matter? *Front Microbiol* **9**: 2850.

Mendes, R., Kruijt, M., de Bruijn, I., Dekkers, E., van der Voort, M., Schneider, J.H. et al. (2011) Deciphering the rhizosphere microbiome for disease-suppressive bacteria. *Science* **332**: 1097-1100.

Mullins, A.J., Murray, J.A.H., Bull, M.J., Jenner, M., Jones, C., Webster, G. et al. (2019) Genome mining identifies cepacin as a plant-protective metabolite of the biopesticidal bacterium *Burkholderia ambifaria*. *Nat Microbiol* **4**: 996-1005.

Naville, M., Ghuillot-Gaudeffroy, A., Marchais, A., and Gautheret, D. (2011) ARNold: a web tool for the prediction of Rho-independent transcription terminators. *RNA Biol* **8**: 11-13.

Newitt, J.T., Prudence, S.M.M., Hutchings, M.I., and Worsley, S.F. (2019) Biocontrol of Cereal Crop Diseases Using Streptomycetes. *Pathogens* **8**: E78.

Nozoe, T., Seto, S., Ito, S., Sato, M., and Katono, T. (1953) Hydroxy derivatives of tropolone, α-thujaplicin and hinokitiol. *Chemical Abstracts* **49**: 8239.

Ossowicki, A., Jafra, S., and Garbeva, P. (2017) The antimicrobial volatile power of the rhizospheric isolate *Pseudomonas donghuensis* P482. *PLoS ONE* **12**: e0174362.

Paterson, J., Jahanshah, G., Li, Y., Wang, Q., Mehnaz, S., and Gross, H. (2017) The contribution of genome mining strategies to the understanding of active principles of PGPR strains. *FEMS Microbiol Ecol* **93**.

Piettre, S.R., Ganzhorn, A., Hoflack, J., Islam, K., and Hornsperger, J.-M. (1997) α-Hydroxytropolones: A New Class of Potent Inhibitors of Inositol Monophosphatase and Other Bimetallic Enzymes. *J Am Chem Soc* **119**: 3201-3204.

Potter, S.C., Luciani, A., Eddy, S.R., Park, Y., Lopez, R., and Finn, R.D. (2018) HMMER web server: 2018 update. *Nucleic Acids Res* **46**: W200-W204.

Reese, M.G. (2001) Application of a time-delay neural network to promoter annotation in the *Drosophila melanogaster* genome. *Computers & Chemistry* **26**: 51-56.

Schubert, M., Lapouge, K., Duss, O., Oberstrass, F.C., Jelesarov, I., Haas, D., and Allain, F.H. (2007) Molecular basis of messenger RNA recognition by the specific bacterial repressing clamp RsmA/CsrA. *Nat Struct Mol Biol* **14**: 807-813.

Sheldrick, G.M. (2015) Crystal structure refinement with SHELXL. *Acta crystallographica Section C, Structural chemistry* **71**: 3-8.

Sievers, F., Wilm, A., Dineen, D., Gibson, T.J., Karplus, K., Li, W. et al. (2011) Fast, scalable generation of high-quality protein multiple sequence alignments using Clustal Omega. *Molecular Systems Biology* **7**: 539.

Solovyev, V., and Salamov, A. (2011) Automatic Annotation of Microbial Genomes and Metagenomic Sequences. In *Metagenomics and its Applications in Agriculture, Biomedicine and Environmental Studies*. Li, R.W. (ed): Nova Science Publishers, pp. 61-78.

Stasiak, J.P., Grigoryan, A., and Murelli, R.P. (2019) Spectrophotometric determination of α-hydroxytropolone pKa values: A structure-acidity relationship study. *Tetrahedron Lett* **60**: 1643-1645.

Taboada, B., Estrada, K., Ciria, R., and Merino, E. (2018) Operon-mapper: a web server for precise operon identification in bacterial and archaeal genomes. *Bioinformatics* **34**: 4118-4120.

Torres, M.J., Brandan, C.P., Petroselli, G., Erra-Balsells, R., and Audisio, M.C. (2016) Antagonistic effects of Bacillus subtilis subsp. subtilis and B. amyloliquefaciens against Macrophomina phaseolina: SEM study of fungal changes and UV-MALDI-TOF MS analysis of their bioactive compounds. *Microbiol Res* **182**: 31-39.

Valverde, C., Heeb, S., Keel, C., and Haas, D. (2003) RsmY, a small regulatory RNA, is required in concert with RsmZ for GacA-dependent expression of biocontrol traits in *Pseudomonas fluorescens* CHA0. *Mol Microbiol* **50**: 1361-1379.

Wang, M.Q., Wang, Z., Yu, L.N., Zhang, C.S., Bi, J., and Sun, J. (2019) Pseudomonas qingdaonensis sp. nov., an aflatoxin-degrading bacterium, isolated from peanut rhizospheric soil. *Arch Microbiol* **201**: 673-678.

Wang, R., Gallant, É., and Seyedsayamdost, M.R. (2016) Investigation of the Genetics and Biochemistry of Roseobacticide Production in the Roseobacter Clade Bacterium *Phaeobacter inhibens*. *MBio* **7**: e02118-e02118.

Xiao, R., and Kisaalita, W.S. (1995) Purification of Pyoverdines of *Pseudomonas fluorescens* 2-79 by Copper-Chelate Chromatography. *Appl Environ Microbiol* **61**: 3769-3774.

Zhou, D., Feng, H., Schuelke, T., De Santiago, A., Zhang, Q., Zhang, J. et al. (2019) Rhizosphere Microbiomes from Root Knot Nematode Non-infested Plants Suppress Nematode Infection. *Microb Ecol* **78**: 470-481.

Table 1. Predicted function of a gene cluster related to the biosynthesis of 7-hydroxytropolone in *Pseudomonas donghuensis* SVBP6. ORFs shaded with the same colour are expected to be encoded within a polycistronic unit (see Figure 1).

ORF	Predicted function	Genbank accession no.	Tn*5* mutant	Best hit ortholog outside *Pseudomonas* spp. (% identity/%coverage) - RefSeq
1	Enoyl-CoA hydratase and related nucleotide-binding proteins (EC 4.2.1.17)	COO64_RS11460		*Azotobacter chroococcum* (73/100) - WP_131340589
2	Universal stress protein A	COO64_RS11465		*Stenotrophomonas rhizophila* (50/98) - AXQ49671
3	Transcriptional regulator, LysR family	COO64_RS11470		*Stenotrophomonas rhizophila* (73/99) - AXQ49670
4	Inner membrane component of tripartite multidrug resistance system	COO64_RS11475		*Stenotrophomonas rhizophila* (78/94) - AXQ49669
5	Membrane fusion component of tripartite multidrug resistance system	COO64_RS11480		*Stenotrophomonas rhizophila* (76/96) - AXQ49668
6	Outer membrane component of tripartite multidrug resistance system	COO64_RS11485	30n, 83j	*Stenotrophomonas rhizophila* (75/96) - AXQ49667
7	Enoyl-(Acyl carrier protein) reductase (EC 1.3.1.9)	COO64_RS11490		*Collimonas sp.* OK242 (76/100) - WP_092359872
8	Alpha-keto-acid decarboxylase; Thiamine pyrophosphate-dependent enzyme (EC:4.1.1.-)	COO64_RS11495		*Paraburkholderia xenovorans* (55/98) - WP_011493090
9	Phenylacetate-coenzyme A ligase (EC 6.2. 1.30)	COO64_RS11500	40b	*Pokkaliibacter plantistimulans* (72/97) - PaaF (WP_104156987)
10	Acyl-CoA dehydrogenase (EC 1.3.2.2)	COO64_RS11505	5n, 16d	*Paraburkholderia sp.* BL21I4N1 (65/98) - WP_105510348
11	4-Hydroxybenzoyl-CoA thioesterase (EC 3.1.2.23)	COO64_RS11510		*Phaeobacter inhibens* (73/99) - TdaD (WP_014881726)
12	Short-chain dehydrogenase/reductase (EC 1.1.1.-)	COO64_RS11515		*Pseudoduganella violaceinigra* (65/98) - WP_083941186
13	HpcH/HpaI aldolase/citrate lyase family (EC 4.1.3.34)	COO64_RS11520		*Pseudoduganella violaceinigra* (65/98) - WP_028103602
14	Transcriptional regulator, TetR family	COO64_RS11525	78i	*Delftia acidovorans* (47/76) - WP_016449798
15	Oxidoreductase, short chain dehydrogenase/reductase family (EC 1.1.1.100)	COO64_RS11530		*Stenotrophomonas rhizophila* (76/100) - AXQ49666

Figure legends

Figure 1. Genomic locus associated with the broad-spectrum antifungal activity of *Pseudomonas donghuensis* strain SVBP6. The diagram shows a 16-kb fragment of the scaffold 5.1 from the draft genome of strain SVBP6. The Tn*5* insertion sites corresponding to six independent isogenic mutants are indicated with white circle-headed lines. Coloured arrows represent the 15 annotated open reading frames within this locus, and their functional assignment is indicated by the coloured boxes at the bottom (Table 1). Dashed arrows represent predicted polycistronic transcripts. The position and orientation of predicted promoters are indicated with bent black arrows. One Rho-independent transcriptional terminator (line tipped with a closed circle) was predicted at the 3' untranslated region of *orf10*. Three putative target mRNA sequences for the post-transcriptional Gac-Rsm cascade were predicted in the complementary strand and their position is indicated with red square-headed lines.

Figure 2. Strain SVBP6 produces a soluble compound compatible with 7-hydroxytropolone. a) UV-visible spectra of culture supernatants of wild type strain SVBP6, a *gacS*::Tn*5* mutant and the Tn*5* mutant 16d, after 8 h of growth in KB medium. b) Relative production of the extracellular compound of the Tn*5* mutants mapping in the genomic region shown in Figure 1, in comparison to wild type strain SVBP6. All cultures were sampled at OD600 ranging 1.7-2.9, and the data are presented as average A327/OD600 values (± standard deviation) for n=3 biological replicates. c) Comparison of the phenotypes of wild type SVBP6, the *gacS*::Tn*5* mutant and the six Tn*5* mutants clustered in the genomic region shown in Figure 1. A327, A393: absorbance at 327 and 393 nm of the corresponding culture supernatants after 8 h of

growth in KB; Pvd: presence of greenish fluorescent pigmentation in culture supernatants after 30 h of growth in KB; *Mp*, *Macrophomina phaseolina*; *Fg*, *Fusarium graminearum*; *Fs*, *Fusarium semitectum*; *Bs*, *Bacillus subtilis* (Table S1). d) Kinetics of production of the extracellular compound (followed as A327 and A393) during growth in KB for the wild type SVBP6 and its isogenic *gacS*::Tn*5* mutant. Each point represents the average of n=3 replicates ± its standard deviation.

Figure 3. **Extraction of metabolites with fungal inhibitory activity from the culture filtrates of *P. donghuensis* strain SVBP6**. a) UV-visible spectra of the culture supernatant in KB medium of strain SVBP6 and its isogenic Tn*5* mutant 16d, with or without addition of the ethyl acetate extract from SVBP6 cultures. b) Representative image of the inhibition test utilized to monitor the activity of the cell-free supernatants and/or of their organic extracts. Each well was inoculated with an agar plug from a fresh PDA plate with confluent growth of *M. phaseolina* isolate CCC 131.2010. The image shown was taken at 3 days after fungal inoculation. Wells that do not contain inhibitory activity show confluent growth of *M. phaseolina* and the presence of black microsclerotia, whereas those wells with varying amounts of inhibitory activity show reduced fungal mycelial growth and absence of microsclerotia (white mycelium). c) Kinetics of *M. phaseolina* growth in the assay depicted in panel b. Each data point corresponds to the average ± standard deviation of the relative area covered by the fungus, for n=3 biological replicates.

Figure 4. **Dose-inhibition curve and stability of the EtOAc organic extract.** a) UV-visible spectra of the tested doses of EtOAc extract that were incorporated into the PDA medium as shown in panel b. b) Representative image of the dose-response assay of the

EtOAc organic extract obtained from the cell-free supernatant of strain SVBP6. The image shown was taken at 3 days after inoculation of wells with *M. phaseolina*. c) Kinetics of *M. phaseolina* growth in the assay depicted in panel b. Each data point corresponds to the average ± standard deviation of the relative area covered by the fungus, for n=3 biological replicates, and the extract doses shown in panel a. d) Kinetics of *M. phaseolina* growth when inoculated at different times (from 0 to 5 days) after pouring the medium containing a fixed amount of 7HT (corresponding to 2× in panel 2c). Each data point corresponds to the average ± standard deviation of the relative area covered by the fungus, for n=3 biological replicates.

Figure 5. **Structure of 7-hydroxytropolone and 2,3-dimethoxy- and 2,7-dimethoxy-tropones.** a) Structure of 7-hydroxytropolone (7HT) produced by *P. donghuensis* SVBP6 (left; R=H), and of the two dimethoxy-tropone derivatives obtained by treatment of 7HT with CH_2N_2 (left, 2,7-dimethoxy-tropone for R=OMe; right, 2,3-dimethoxy-tropone). b) ORTEP view of the 7HT crystal obtained from the EtOAc extract of the cell-free supernatant from SVBP6 cultures in KB medium (see crystal data in Supplementary Table 2). Thermal ellipsoids were drawn at 30% probability level.

Figure 6. Fungal inhibitory activity of 7HT and its dimethoxy derivatives. a) UV-visible spectra of KB medium containing either the EtOAc extract from SVBP6 culture supernatant or purified 7HT. b) Kinetics of *M. phaseolina* growth in the presence of the EtOAc extract from wild type SVBP6, purified 7HT or its 2,3-dimethoxy- or 2,7-dimethoxy-tropones (Figure 5a), all at equivalent micromolar concentrations. Each data

point corresponds to the average ± standard deviation of the relative area covered by the fungus, for n=3 biological replicates.

Figure 7. **Iron effect on production of 7HT and antifungal activity of strain SVBP6**. a) Production of 7HT (estimated as A327 nm) in the presence of different supplement concentrations of $FeSO_4$. The OD600 of cultures at the moment of sampling and the A327 of the cell-free supernatants are presented as average values ± standard deviation for n=3 biological replicates. b) Kinetics of *M. phaseolina* growth in the presence of different 7HT and $FeSO_4$ concentrations. Each data point corresponds to the average ± standard deviation of the relative area covered by the fungus, for n=3 biological replicates.

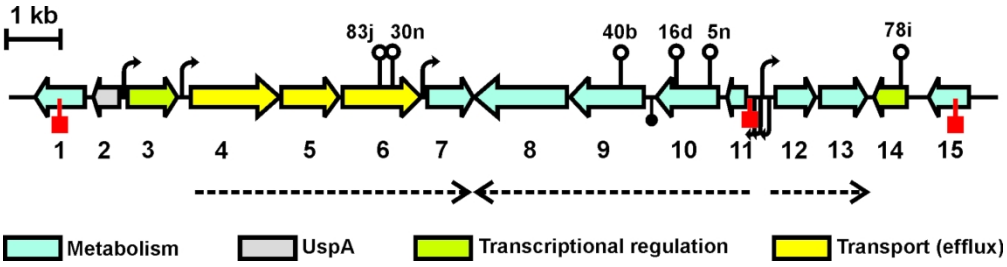

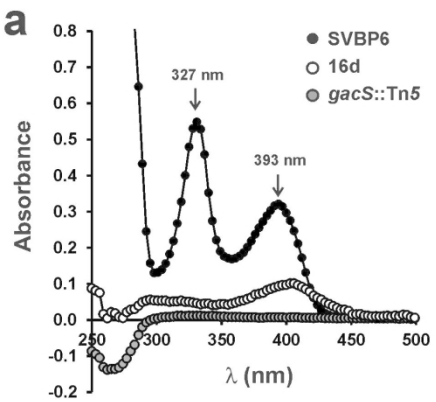

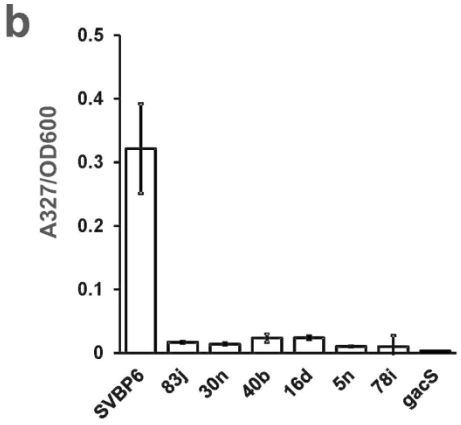

c

	A327	A393	Pvd	Inhibition of *Mp*	*Fg*	*Fs*	*Bs*
wild type	0.51	0.35	+	+	+	+	+
83j	0.03	0.01	-	-	-	-	+
30n	0.04	0.07	+	-	-	-	+
40b	0.05	0.08	+	-	-	-	+
16d	0.05	0.09	+	-	-	-	+
5n	0.03	0.06	+	-	-	-	+
78i	0.02	0.06	+	-	-	-	n.d.
gacS::Tn*5*	0.01	0.01	+	-	-	-	-

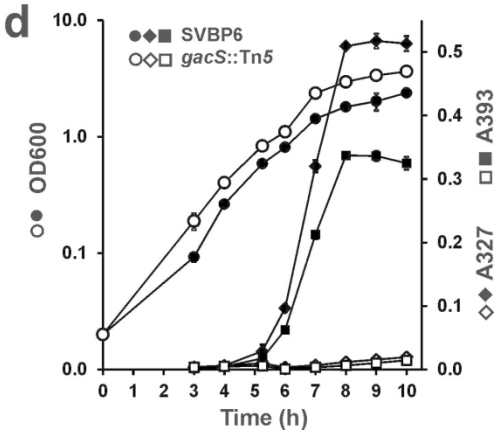

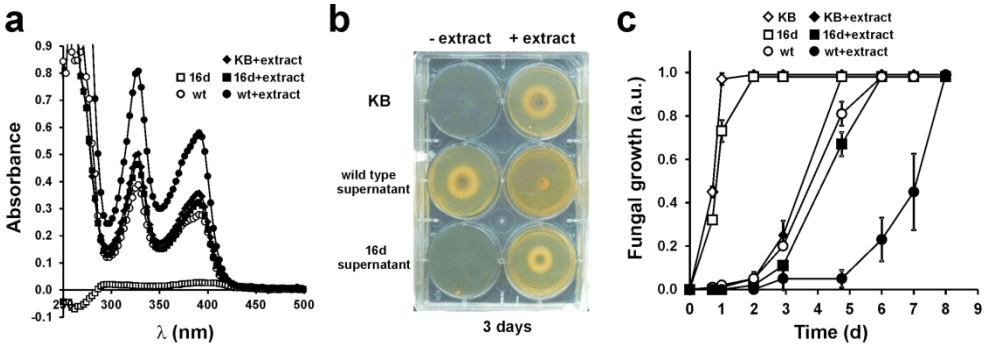

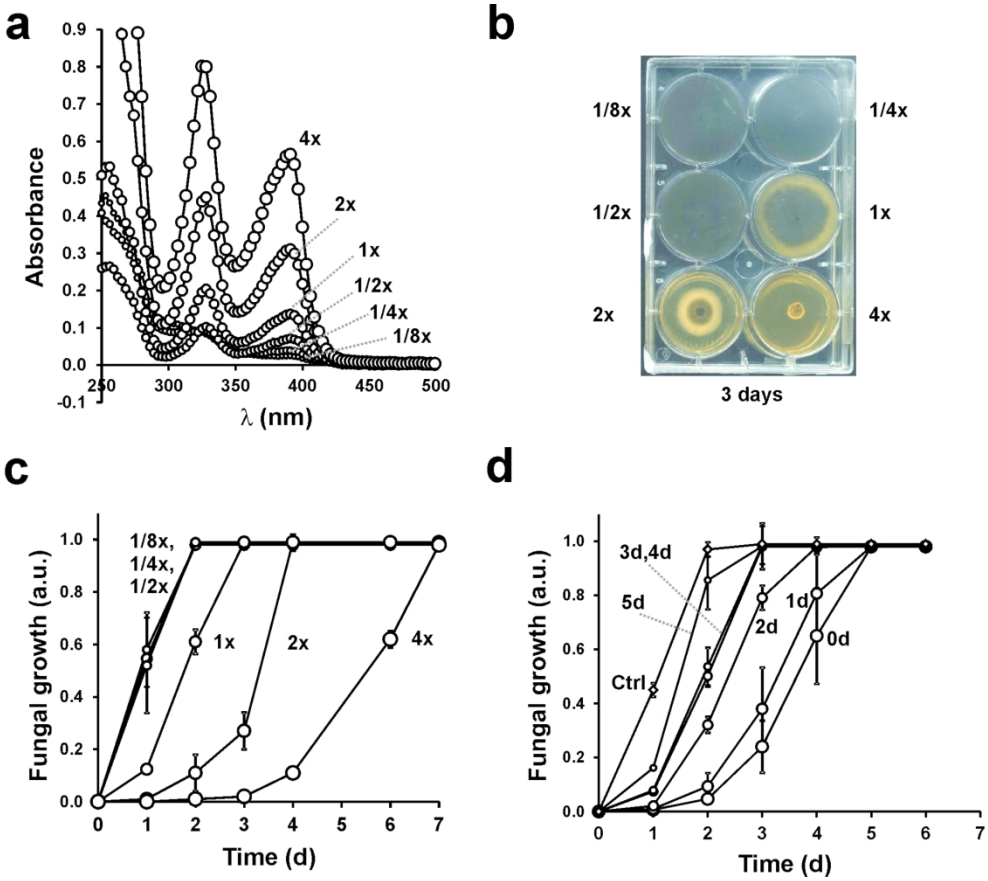

a

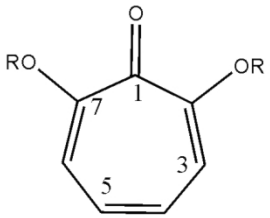

7-Hydroxytropolone, R=H
2,7-Dimethoxytropone, R=Me

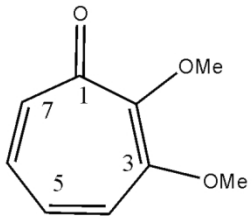

2,3-Dimethoxytropone

b